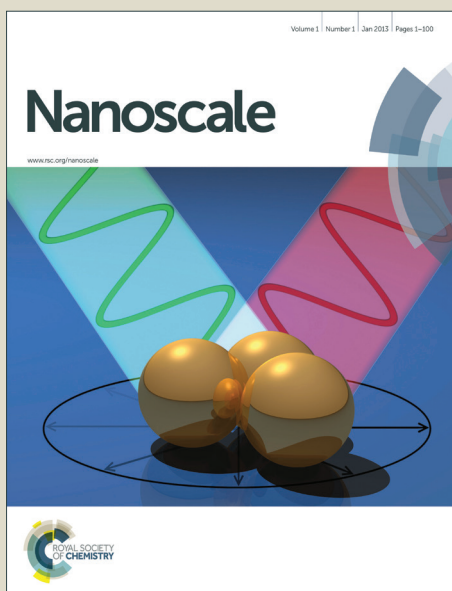


# Nanoscale

Accepted Manuscript



This is an *Accepted Manuscript*, which has been through the Royal Society of Chemistry peer review process and has been accepted for publication.

*Accepted Manuscripts* are published online shortly after acceptance, before technical editing, formatting and proof reading. Using this free service, authors can make their results available to the community, in citable form, before we publish the edited article. We will replace this *Accepted Manuscript* with the edited and formatted *Advance Article* as soon as it is available.

You can find more information about *Accepted Manuscripts* in the [Information for Authors](#).

Please note that technical editing may introduce minor changes to the text and/or graphics, which may alter content. The journal's standard [Terms & Conditions](#) and the [Ethical guidelines](#) still apply. In no event shall the Royal Society of Chemistry be held responsible for any errors or omissions in this *Accepted Manuscript* or any consequences arising from the use of any information it contains.

## COMMUNICATION

## Covalent Attachment and Growth of Nanocrystalline Films of Photocatalytic TiOF<sub>2</sub>

Cite this: DOI: 10.1039/x0xx00000x

Jian Zhu,<sup>‡a</sup> Fujian Lv,<sup>‡a</sup> Shengxiong Xiao,<sup>a</sup> Zhenfeng Bian,<sup>a</sup> Gerd Buntkowsky,<sup>c</sup> Colin Nuckolls<sup>\*a,b</sup> and Hexing Li<sup>\*a</sup>

Received 00th January 2012,  
Accepted 00th January 2012

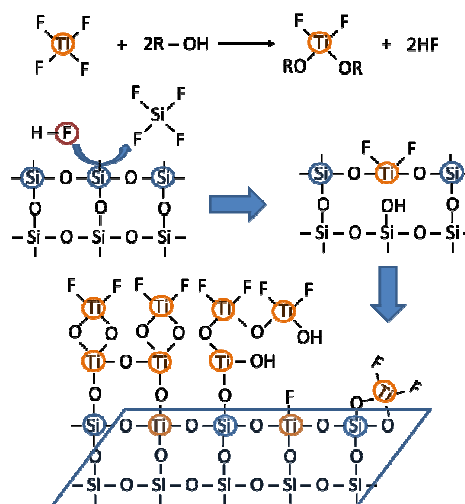
DOI: 10.1039/x0xx00000x

www.rsc.org/

**This manuscript describes a synthesis of nanocrystalline TiOF<sub>2</sub> film. The nanocrystalline TiOF<sub>2</sub> becomes chemically attached to the surface of the glass slide. These films are robust and can be recycled as photocatalysts for the degradation of organic dyes and solvents. These films also have significant antibacterial properties upon irradiation.**

The main text of the article should go here with headings as appropriate. We describe here a method to synthesize and grow robust, nanostructured photocatalytic semiconductor films on glass surfaces. The abundance of energy from the sun makes photocatalysis attractive for numerous applications such as environmental remediation,<sup>1-3</sup> H<sub>2</sub> production,<sup>4, 5</sup> and “green” reaction chemistry.<sup>6-9</sup> The most well studied systems utilize films of TiO<sub>2</sub>. TiO<sub>2</sub> films have been created by numerous methods including vacuum evaporation, magnetron sputtering, chemical vapor deposition, plasma spraying, and sol-gel methods and studied as photocatalysts.<sup>10-13</sup> TiO<sub>2</sub> is a wide bandgap semiconductor and that is only activated by UV irradiation.<sup>14, 15</sup> To narrow the band gap, a common strategy is to dope the TiO<sub>2</sub>, but this has the unwanted effect of the dopants often leaching out of the films.<sup>16-18</sup> Many alternative thin film semiconductors have band gaps that provide more overlap with the solar emission spectrum, but they suffer from poor activity due to the low surface area of the film.<sup>19-22</sup> To create films that are both durable and have high surface area, it is important to avoid calcination<sup>23, 24</sup> but still form a robust and intimate contact between the semiconductor thin film and the substrate. We recently reported a method to make polycrystalline TiOF<sub>2</sub> by an aerosol technique. Made by this method, the TiOF<sub>2</sub> had high activity in photocatalytic degradation of organic compounds under visible light irradiation.<sup>25</sup> TiOF<sub>2</sub> has a narrower band gap than TiO<sub>2</sub> and avoids the problems associated with fluoride leaching from fluoride doped TiO<sub>2</sub>. Here we describe, for the first time, a method for the in situ growth of mesoporous films of nanocrystals of TiOF<sub>2</sub> that are covalently attached to the glass

substrate. Because of the bonding between the TiOF<sub>2</sub> films and the substrate, this system is durable and can be recycled many times as photocatalysts for degradation of organic pollutants and for antimicrobial behaviour in films.



**Scheme 1.** Formation process of TiOF<sub>2</sub> film on the glass surface.

We developed an evaporation induced alcoholysis (EIA) method that utilizes TiF<sub>4</sub> in an ethanol solution to react with glass substrates to create the mesoporous, nanocrystalline films of TiOF<sub>2</sub>. The TiOF<sub>2</sub> films are covalently bonded to the substrate. This study is based on the method of SiO<sub>2</sub> synthesis developed by Guglielmi and Zenezini.<sup>26</sup> To create the films, we immersed glass substrates into a solution of TiF<sub>4</sub> in ethanol (5 minutes, 25 °C) and then dried the samples for 24 h at 100 °C. We varied the thickness of the films by adjusting TiF<sub>4</sub> concentration in the ethanol solution (from 0.10, 0.20, 0.30, 0.40 to 0.50 M). We labeled the films as T1 (0.10 M reaction

mixture) to T5 (0.50 M reaction mixture) based on the concentration of  $\text{TiF}_4$  used to produce them.

We monitor this process by  $^{19}\text{F}$  NMR spectroscopy (Fig. S1). In the initial period of the reaction (1.5 h), we observe three kinds of  $^{19}\text{F}$  resonances:  $\text{TiF}_4$  (319 ppm),  $(\text{RO})_2\text{TiF}_2$  (257 ppm) and  $(\text{RO})_3\text{TiF}$  (75 ppm).<sup>27-30</sup> In addition, we observe a small peak  $-53$  ppm that is from  $\text{HF}^{31}$  in ethanol. After 5 h, the intensities of all those resonances decrease abruptly due to further alcoholysis, and a new signal appears around  $-32$  ppm, corresponding to the  $^{19}\text{F}$  species of  $\text{TiOF}_2$ . Furthermore, the resonance from  $\text{SiF}_4$  appears at  $-60$  ppm. After 24 h, we observe only the resonance at  $-32$  ppm, suggesting the complete alcoholysis of organic Ti precursors into  $\text{TiOF}_2$ . We hypothesize, and demonstrate here, that the evaporation of ethanol induces the alcoholysis of  $\text{TiF}_4$  to  $(\text{RO})_2\text{TiF}_2$  that reacts with the hydroxyl groups on the glass leading to a film of  $\text{TiOF}_2$ . Meanwhile, the HF produced from the  $\text{TiF}_4$  alcoholysis etches the glass surface leaving silicon vacancies that are occupied by titanium. The end result is an interface between the  $\text{TiOF}_2$  film and glass substrate that has Ti-O-Si bonds. This process is displayed in Scheme 1. We also used different solvents, such as water and tetra. butyl alcohol instead of ethanol, only  $\text{TiOF}_2$  could be obtained. The possible reason is that  $(\text{RO})_2\text{TiF}_2$  is more stable than other intermediate products.

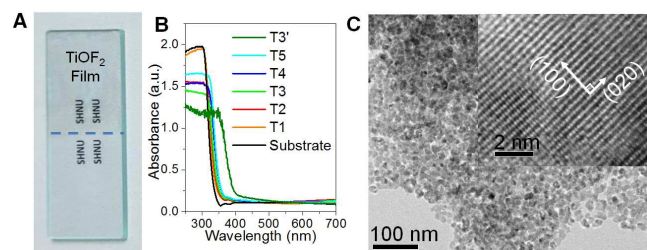


**Fig. 1** (A) Transparent film of T3 on a glass substrate. (B) UV-vis DRS spectra for films and particles of  $\text{TiOF}_2$ . (C) TEM image of T3. Inset: high resolution TEM image of T3.

The optical photo shows that all of the films are transparent to the eye (Fig. 1A). The films are smooth (Fig. S2A); Atomic force microscopy (Fig. S2B) indicates that for T3 the RMS roughness is 2.1 nm. Fig. 1B shows the light absorbance spectra for T1–T5 obtained using UV-Vis diffuse reflectance spectroscopy. T1–T5 demonstrates low visible light adsorption due to the smooth surface with low diffuse reflectance. The T3' particle scraped from T3 film exhibits the intrinsic highest absorbance for visible light.

We can index the X-ray diffraction patterns from these films (see supporting information Fig. S3) to a cubic  $\text{TiOF}_2$  crystal (JCPDS card No. 08-0060) based on the (100), (200), and (210) reflections. From the Scherrer equation, the  $\text{TiOF}_2$  crystal size is  $\sim 25$  nm. From transmission electron microscopy (Fig. 1C), the film contains nanoparticles with an average size about  $20 \pm 2$  nm. The high resolution TEM image (the inset to Fig. 1C) contains two kinds of perpendicularly arranged lattice fringes, corresponding to the vertically crossed (100) and (020) facets of the cubic  $\text{TiOF}_2$  nanocrystals.

Fig. 2A-E displays the cross-section FESEM images for the films T1-T5. The film thickness increases linearly based on the amount of  $\text{TiF}_4$  in the reaction condition. The thinnest of the films, T1, is  $125 \pm 5$  nm thick, and the thickest, T5, is  $460 \pm 10$  nm. Elemental mapping of the interface in these cross sectional samples (Fig. 1F) shows Ti on the surface of the film and Si on the interior of the film with an interface between them. For the elemental mapping of T3, the depth of the Ti film is  $\sim 350 \pm 10$  nm. This thickness agrees with the  $319 \pm 8$  nm measured from the cross sectional SEM image. At the interface, the Ti and Si elements overlap each other. This implies that there is a strong interaction between  $\text{TiOF}_2$  film and the glass surface through the formation of Ti-O-Si bonds. The Ti : O : F atomic ratio from EDX analysis is (1 : 1.3 : 1.9). The slightly higher oxygen content is from the  $\text{SiO}_2$  glass substrate, and the lower fluorine is from the formation of the O-Si-O-Ti-O bonds instead of F-Ti-O at interface (as in Scheme 1).

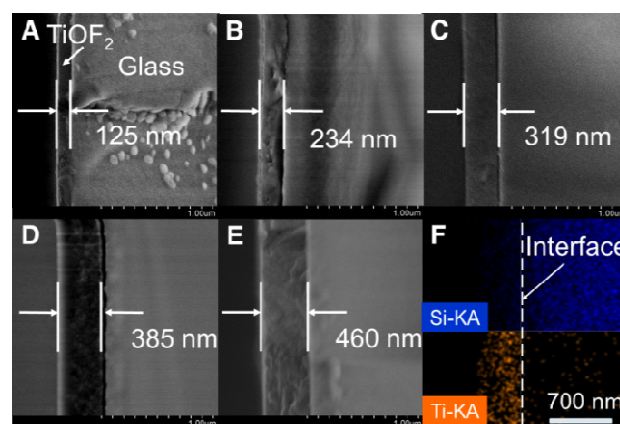


**Fig. 2** (A-E) Cross-section FESEM images for the films T1-T5. (F) Elemental mapping of the silicon and titanium atoms at the interface between the glass and  $\text{TiOF}_2$  nanocrystalline films.

To further investigate the interface and bonding between the glass and  $\text{TiOF}_2$ , we performed XPS depth profiling. Details of this can be found in the Supporting Information. The XPS spectra (Fig. 3) confirm the formation of  $\text{TiOF}_2$  on the surface of the glass substrate with binding energy (BE) of 686.0 eV for the F 1s and 531.4 eV for the O 1s levels. At a depth of 350 nm, we find a new silicon containing species that is indicative of a Si-O-Ti bond with a BE of 104.0 eV.<sup>32, 33</sup> More interesting, such method has also been successfully applied on the ITO glass substrate in preparing the  $\text{TiOF}_2$  covered ITO electrode. The XPS spectra (Fig. S4) show different case comparing to pure glass substrate. The  $\text{TiOF}_2$  has interaction with In and Sn species instead of Si species, due to the slight shift of binding energy of F 1s and Ti 2p with the increasing depth. At a depth of 400 nm, there is no F, Ti species have been found. The possible reason is that formed acid product can corrode In-O and Sn-O species and induce the formation of Ti-O-In or Ti-O-Sn, similar to the process on pure glass substrate. And Si species has been found at depth of 500 nm, further confirming that there is no direct reaction between  $\text{TiOF}_2$  and Si species. It confirms that

the nanocrystalline TiOF<sub>2</sub> is chemically bonded to the both glass and ITO substrate.

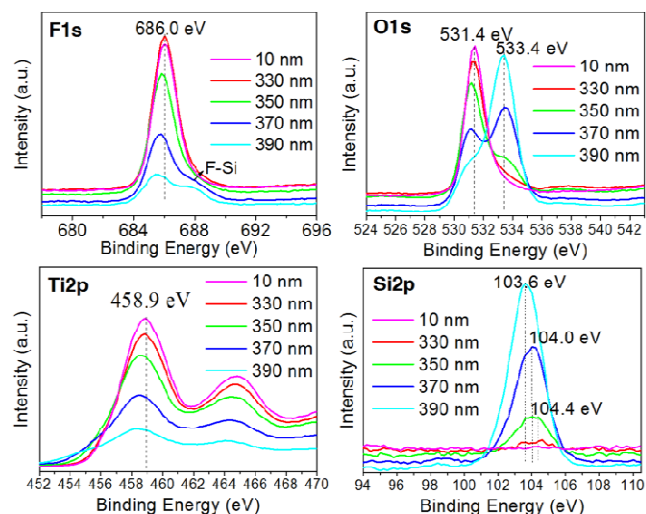


**Fig. 3** XPS spectra of T3 sample at different film depths obtained by adjusting Ar<sup>+</sup> etching time.

To test the properties of these films, we investigated them for the photocatalytic degradation of both aqueous rhodamine B (RhB) and gaseous acetone. For the RhB degradation we used a monochromatic light source with a wavelength ( $\lambda$ ) of  $435 \pm 20$  nm to avoid sensitization of the RhB molecules. For the photocatalytic degradation of acetone, we used a visible light source of  $\lambda > 420$  nm (see the Supporting Information for experimental details). All of the films were active as photocatalysts. The activity of the films is summarized in Table 1. T3 exhibits the highest activity in both the liquid phase photocatalytic degradation of RhB and the gas phase photocatalytic degradation of acetone (see Fig. S4). The similar result has been found in the degradation of other dyes such as methylene blue and fuchsin basic (see Fig. S6). As a comparison, the pure TiO<sub>2</sub> film prepared by sol-gel method has been applied in degradation of RhB, and only decolorization rate of 8% was detected. The extremely low activity of the pure TiO<sub>2</sub> film could be attributed to the big energy band gap of TiO<sub>2</sub> (3.0~3.2 eV), which could not be activated by visible lights. We also found that these films have significant antibacterial properties against *Staphylococcus aureus* under visible light irradiation (See Supporting Information and Fig. S7 for experimental details)

**Table 1** Structural parameters and photocatalytic performance.<sup>a</sup>

Samples	S <sub>BET</sub> (m <sup>2</sup> /g)	D <sub>p</sub> (nm)	V <sub>p</sub> (cm <sup>3</sup> /g)	Decolorization Rate (%)
T1	47	2.3	0.066	61
T2	75	2.5	0.17	80
T3	84	2.3	0.20	92
T4	72	2.5	0.15	82
T5	22	2.5	0.076	76

<sup>a</sup>Reaction conditions: 28 cm<sup>2</sup> TiOF<sub>2</sub> film on petri dish, 5.0 mL 10 ppm RhB aqueous solution, a 300 W Xe lamp with wavelength of  $435 \pm 20$  nm, 10°C, 6 h.

An important consideration for film-based photocatalysts is their reusability. Fig. 4A shows the recycling test of the T3 during liquid phase photocatalytic degradation of RhB under visible light irradiation. T3 was used repetitively without any decrease in activity. We attribute the durability of this film to the covalent attachment at the interface between the TiOF<sub>2</sub> film and the glass substrate. To highlight the stability of the covalently bonded films we treated T3 to ultrasonication. There was no detectable leaching of TiOF<sub>2</sub> from the T3 film after 90 minutes of sonication. Even extend sonication time to 180 min, there is only 0.5% weight loss could be detected.

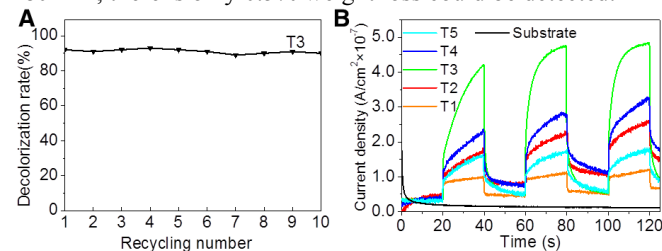


**Fig. 4** (A) Recycling test for T3 photocatalytic degradation of RhB (B) Visible light ( $\lambda > 420$  nm) induced photocurrent profiles for the films T1-T5.

We investigated the structure of the films to determine the origin of the high photocatalytic behaviour of T3 relative to the other films. T3 has the strongest visible light induced photocurrent (Fig. 4B) that may result from the higher surface area and appropriate thickness facilitating the electron transfer. We also found that all the films have a mesoporous structure that has a type IV N<sub>2</sub> adsorption-desorption isotherm. Such mesoporous structures are commonly observed in inorganic materials synthesized by alcoholysis owing to the presence of alcohol templates.<sup>34</sup> Using Brunauer-Emmett-Teller and Barrett-Joyner-Halenda models on the desorption branches of the N<sub>2</sub> adsorption-desorption isotherms, we calculate the surface area (S<sub>BET</sub>), average pore diameter (D<sub>p</sub>) and pore volume (V<sub>p</sub>). As shown in Table 1, T1-T5 samples display high S<sub>BET</sub> and similar D<sub>p</sub> owing to the mesoporous structure. The S<sub>BET</sub> and V<sub>p</sub> increases gradually from T1 to T3 owing to the enhanced content of TiOF<sub>2</sub> film on the glass substrate. However, when the TiOF<sub>2</sub> film is made thicker there is a rapid decrease in S<sub>BET</sub> and V<sub>p</sub>. The thicker films may occlude access to the pores.

In summary, we have developed a general and facile approach for synthesizing and the *in situ* bonding of nanocrystalline TiOF<sub>2</sub> to form transparent, mesoporous films on glass substrates. These films show high activity in the photocatalytic degradation of aqueous RhB and gaseous acetone that is dependent on the structured nanocrystals in the active layer. Moreover, these films show significant antibacterial properties under visible light irradiation. Given the simplicity of this approach it can be applied to the *in situ* transparent coating of TiOF<sub>2</sub> film onto other common glass-based substrates (see Fig. S8). These results chart a path to applications in air and water remediation.

## Acknowledgements

This material is based upon work supported by the NSF of China (21237003, 21261140333, 21377088), Shanghai Government (13ZR1430600, 14ZZ126), Program for Changjiang Scholars and Innovative Research Team in University (PCSIRT, IRT1269), the Program for Professor of Special Appointment (Eastern Scholar) at Shanghai Institutions of Higher Learning (No.2013-57), CN was primarily supported by the Center for Re-Defining Photovoltaic Efficiency Through Molecular-Scale Control, an Energy Frontier Research Center funded by the U.S. Department of Energy (DOE), Office of Science, Office of Basic Energy Sciences under award number DE - SC0001085. We thank Yeping Xu (TU Darmstadt) for NMR analysis.

## Notes and references

<sup>a</sup> Chinese Education Ministry Key Lab of Resource Chemistry and Shanghai Key Laboratory of Rare Earth Functional Materials, Shanghai Normal University, Shanghai, 200234, CHINA. Email: hexing-li@shnu.edu.cn.

<sup>b</sup> Department of Chemistry, Columbia University, New York, NY 10027, USA. Email: cn37@columbia.edu.

<sup>c</sup> Eduard-Zintl-Institut für Anorganische und Physikalische Chemie Technische Universität Darmstadt, Petersenstr. 2064287, GERMANY.

† Electronic Supplementary Information (ESI) available: [Methods for sample preparation, characterization and Figures S1–S8]. See DOI:10.1039/c000000x/

\* These authors contributed equally.

- 1 K. Ramamoorthy, K. Kumar, R. Chandramohan and K. Sankaranarayanan, *Mater. Sci. Eng. B*, 2006, **126**, 1-15.
- 2 K. Samedov, Y. Aksu and M. Driess, *ChemPlusChem*, 2012, **77**, 663-674.
- 3 T. R. Bao Foong, S. P. Singh, P. Sonar, Z. E. Ooi, K. L. Chan and A. Dodabalapur, *J. Mater. Chem.*, 2012, **22**, 20896-20901.
- 4 J. Zhang, J. Yu, Y. Zhang, Q. Li and J. R. Gong, *Nano Lett.*, 2011, **11**, 4774-4779.
- 5 J. Wang, P. Zhang, X. Li, J. Zhu and H. Li, *Appl. Catal. B*, 2013, **134-135**, 198-204.
- 6 T. P. Yoon, M. A. Ischay and J. Du, *Nat. Chem.*, 2010, **2**, 527-532.
- 7 G. Palmisano V., Augugliaro, M. Pagliaro and L. Palmisano, *Chem. Commun.*, 2007, **33**, 3425-3437.
- 8 J. Zhao, Z. Zheng, S. Bottle, A. Chou, S. Sarina and H. Zhu, *Chem. Commun.*, 2013, **49**, 2676-2678.
- 9 J. Wang, Z. Bian, J. Zhu and H. Li, *J. Mater. Chem. A*, 2013, **1**, 1296-1302.
- 10 L. Di, X. Li, C. Shi, Y. Xu, D. Zhao and A. Zhu, *J. Phys. D*, 2009, **42**, 32001-32004.
- 11 H. J. Moon, S. Baumann, S. Uhlenbruck, D. Sebold, W. A. Meulenber and H. Park, *Thin Solid Films*, 2012, **526**, 59-64.
- 12 J. Yu, X. Zhao and Q. Zhao, *Mater. Chem. Phys.*, 2001, **69**, 25-29.
- 13 G. Abellan, E. Coronado C., Marti-Gastaldo, A. Ribera, J. F. Sanchez-Royo, *Chem. Sci.*, 2012, **3**, 1481-1485.
- 14 A. K. P. D. Savio, J. Fletcher and H. F. C. Robles, *Ceram. Int.*, 2013, **39**, 2753-2765.

- 15 G. Liu, L. C. Yin, J. Wang, P. Niu, C. Zhen, Y. Xie and H. M. Cheng, *Energy Environ. Sci.*, 2012, **5**, 9603-9610.
- 16 P. Romero-Gómez, S. Hamad, J. C. González, A. Barranco, J. P. Espinós, J. Cotrino and A. R. González-Elipé, *J. Phys. Chem. C*, 2010, **114**, 22546-22557.
- 17 H. X. Li, X. Y. Zhang, Y. N. Huo, J. Zhu, *Environ. Sci. Technol.*, 2007, **41**, 4410-4414.
- 18 C. Han, M. Pelaez, V. Likodimos, A. G. Kontos, P. Falaras, K. O'Shea, and D. D. Dionysiou, *Appl. Catal. B*, 2011, **107**, 77-87.
- 19 X. Li, R. Huang, Y. Hu, Y. Chen, W. Liu, R. Yuan and Z. Li, *Inorg. Chem.*, 2012, **51**, 6245-6250.
- 20 O. Hameit and H. J. Müller-Buschbaum, *Alloys Comp.*, 1993, **194**, 101-103.
- 21 J. Ye, Z. Zou, H. Arakawa, M. Oshikiri, M. Shimoda, A. Matsushita and T. Shishido, *J. Photochem. Photobiol. A*, 2002, **148**, 79-83.
- 22 T. Su, H. Jiang and H. Gong, *J. Solid State Chem.*, 2011, **184**, 2601-2604.
- 23 R. J. Davis and Z. Liu, *Chem. Mater.*, 1997, **9**, 2311-2324.
- 24 C. He, B. Tian and J. J. Zhang, *Colloid Inter. Sci.*, 2010, **344**, 382-389.
- 25 J. Zhu, D. Zhang, Z. Bian, G. Li, Y. Huo, Y. Lu, H. Li, *Chem. Commun.*, 2009, **36**, 5394-5396.
- 26 M. Guglielmi and S. Zenezini, *J. Non-Cryst. Solids*, 1990, **121**, 303-309.
- 27 C. B. C. Nobrega, F. Y. Fujiwara, J. A. Cury and P. L. Rosalen, *Chem. Pharm. Bulletin*, 2008, **56**, 139-141.
- 28 D. S. Dyer and R. O. Ragsdale, *J. Am. Chem. Soc.*, 1967, **89**, 1528-1529.
- 29 T. S. Cameron, A. Decken, E. G. Ilyin, G. B. Nikiforov and J. Passmor, *Eur. J. Inorg. Chem.*, 2004, **19**, 3865-3872.
- 30 R. O. Ragsdale and B. B. Stewart, *Inorg. Chem.*, 1963, **2**, 1002-1004.
- 31 K. O. Christe and W. W. Wilson, *J. Fluorine Chem.*, 1990, **46**, 339-342.
- 32 E. Pabón, J. Retuert, R. Quijada and A. Zarate, *Microporous Mesoporous Mater.*, 2004, **67**, 195-203.
- 33 F. Garbassi and L. Balducci, *Microporous Mesoporous Mater.*, 2001, **47**, 51-59.
- 34 J. Zhu, J. Ren, Y. Huo, Z. Bian and H. Li, *J. Phys. Chem. C*, 2007, **111**, 18965-18969.